Lawrence Berkeley Laboratory
UNIVERSITY OF CALIFORNIA

Materials & Molecular
Research Division

Submitted to Acta Metallurgica

DEFORMATION AND FAILURE CAUSED BY GRAIN BOUNDARY SLIDING AND BRITTLE CRACKING

Anthony G. Evans

December 1979

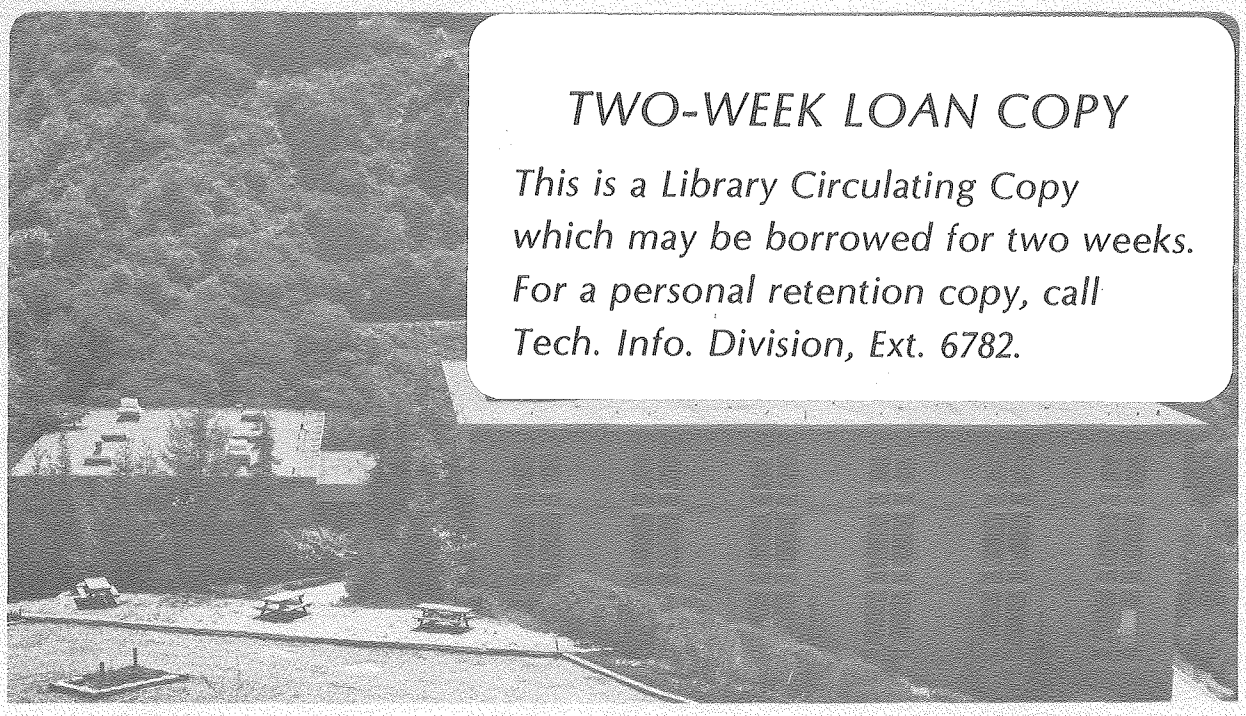

Prepared for the U.S. Department of Energy under Contract W-7405-ENG-48

DISCLAIMER

DEFORMATION AND FAILURE CAUSED BY GRAIN BOUNDARY SLIDING AND BRITTLE CRACKING

Anthony G. Evans
Lawrence Berkeley Laboratory
Materials Science and Mineral Engineering
University of California, Berkeley
Berkeley, CA 94720

ABSTRACT

A failure mechanism which entails grain boundary sliding and brittle crack extension along grain boundaries is analyzed. It is demonstrated that the crack growth, which occurs above a threshold stress, is dictated by the grain boundary viscosity, fracture energy, the grain facet length, and the boundary orientations vis-a-vis the applied stress. The time taken to form a stable facet-sized crack is derived, and shown to be non-linear in the applied stress. The creep strains that result from this mode of cracking are generally small and non-linear.

DEFORMATION AND FAILURE CAUSED BY GRAIN BOUNDARY SLIDING AND BRITTLE CRACKING

A. G. Evans

I. INTRODUCTION

Cracks or cavities freqently form during the creep deformation of ceramics and metals. The propagation of individual cavities or cavity arrays, either by diffusion[1-5] or by viscous flow[6] of a boundary phase, has attained an advanced level of comprehension. The coupled cavity propagation, coalescence effects that dictate the final failure have also been examined,[7] using statistical methods; although these developments are at an elementary level. The intent of the present paper is to examine brittle crack extension as an alternate mechanism of creep fracture.

Several authors have examined the problem of brittle cracking along grain boundaries during creep.[8-11] These studies have generally commenced from the premise that grain boundary sliding will be occurring (during steady state creep) at a specified rate, $\dot{u}_{g.b.s}$, and that the resultant sliding displacements provide the impetus for extension of a brittle wedge crack (Fig. 1). However, a prescribed steady state grain boundary sliding can only be occurring if the sliding is everywhere accommodated either by diffusion[12] or, perhaps, by cracking. If it is implicitly assumed that diffusional accommodation is occurring, then it must be appreciated that diffusion will also modity the configuration of the crack tip.[1-3] In fact, the crack (which becomes a cavity) will extend by diffusion, in accord with the descriptions outlined by

Chuang, et al,[1,4] Vitek[2] and Speight et al.[3] The earlier models[8-10] used linear elastic wedge opening solutions to describe the crack length and are thus not pertinent to conditions which involve diffusion. The presence of a steady state boundary sliding displacement to extend the crack is thus ambivalent. It was subsequently recognized[11] that a wedge crack, once initiated, is likely to extend by diffusion, whenever diffusive conditions exist; and an approximate analysis of diffusive extension was presented. A more detailed analysis based on recent 'crack-like' cavity extension concepts[1-3], needed to afford a thorough description of the failure process, will be presented in a subsequent publication.[13]

In the present analysis diffusion is not admitted and the only permissible viscous motion is grain boundary sliding. Brittle cracks are then tenable. The occurrence of this condition must be limited (since grain boundary sliding itself usually involves diffusive processes, because of the presence of ledges and of non-planarity), but important situations can be conceived wherein the proposed process might be encountered. For example, ceramics prepared by liquid phase sintering (e.g., Si_3N_4) often have planar boundaries, and contain a second phase at the boundaries that is too narrow (a few lattice spacings) to admit viscous modifications of the crack tip but wide enough to facilitate boundary sliding.[14,15]

The analysis of crack extension along individual grain boundary facets is followed by an examination of both the creep strains that can be induced by this cracking process and the resultant failure times. It is demonstated that the creep strain rates are generally small and non-linear.

2. THE CRACK EVOLUTION SEQUENCE

If diffusion or viscous flow are excluded, grain boundary sliding will result in elastic stress concentrations at grain triple points.[16,17] The stress concentration in the absence of plasticity has the square root singularity, typical of shear cracks. A crack will develop from the triple point either if the singularity attains the critical level required for grain boundary fracture, $K_c^{g.b}$, or if a defect of sufficient size pre-exists at the grain boundary. The onset of cracking will thus depend on the local conditions at individual triple points.

The presence of the crack will relax the elastic stress concentration at the triple point and permit the adjacent boundaries to slide: thereby producing an opening displacement at one end of the crack. As the sliding progresses, the stress intensity factor at the micro-crack tip increases, causing additional crack extension and further sliding (Fig. 1). Also, the stress concentration at the neighboring triple points becomes enhanced, leading to an increased probability of micro-crack initiation at these locations. Once the crack reaches the opposing triple point, the singularity at its tip will begin to relax, by sliding of the intersecting boundaries (Fig. 1), and further crack extension will be suppressed. The ultimate formation of open facet-sized cracks is thus to be anticipated. Failure will presumably occur when sufficient contiguous boundaries have developed cracks to form a macro-crack of critical size.[7] The interaction of propagating cracks with preformed cracks is thus undoubtedly involved in the failure process.

3. STRESS INTENSITY FACTOR SOLUTIONS

The extension of a wedge crack that emanates at a triple point has previously been analyzed using a cracked dislocation solution, first

proposed by Stroh[18] and extended by Cottrell.[19] This solution can be demonstrated (Appendix I) to exhibit the form;

$$K \approx \sigma_n \sqrt{\pi(a/2)} + hE/\sqrt{2\pi a} \quad (1-\nu^2) \tag{1}$$

where 2h is the wedge opening, a is the crack length, K is the stress intensity factor, E is Young's modulus and σ_n is the component of the applied stress normal to the crack. The first term is due to the normal opening of the crack K_σ and the second derives from the wedge opening produced by sliding, K_w. However, this solution is inadequate for the complete description of the wedge crack extension; because the wedge opening h cannot be specified a priori (steady state sliding will not occur in the present problem). A companion solution that provides the requisite complementary information can be derived from recent stress intensity solutions for the kinked crack,[20] with the kink at an inclination ϕ to the sliding boundary (Fig. 2). The pertinent stress intensity factors are deduced by regarding the primary crack as being subjected to a pure shear stress τ (Fig. 2) plus a small superimposed crack surface traction to prevent opening of the primary crack (Fig. 2). The mode I and II stress intensity factors provided by the analysis are then combined in accord with the coplanar strain energy release rate criterion to obtain the driving force K^τ for coplanar wedge crack extension, as;

$$K^\tau = [K_I^2 + K_{II}^2]^{\frac{1}{2}} \tag{2}$$

The results, plotted in terms of the normalized stress intensity factor

$K^T (=K^T/\tau\sqrt{\ell})$, are shown in Fig. 2 for several inclinations, ϕ. There is an equivalent enhancement of the mode II stress intensity factor at the other triple point. For applied stress conditions other than pure shear parallel to the sliding boundary, the important stresses are the shear stress resolved along the boundary τ_s and the normal stress that induces an additional wedge crack opening. Information concerning the relation between h/a and $\tau_s\sqrt{\ell}$ can clearly be extracted from a detailed comparison of the two solutions. However, this is not required for present purposes.

Comparing K from Fig. 2 with the critical value for grain boundary fracture $K_c^{g.b}$ (Fig. 3) permits the prerequisites for crack formation on a specific facet (as well as the ultimate wedge crack extension on that facet) to be specified. Thereafter, the rate of crack extension on the susceptible boundaries can be determined, as demonstrated in the following section. The susceptibility of a boundary to cracking is simply ascertained by comparing K at $(a/\ell) = 0$ (referred to as K_o) with $K_c^{g.b}$. Those boundaries for which $K_o > K_c^{g.b}$ will exhibit an instantaneous tendency for crack initiation. Then, for those grain orientations in which K decreases as a/ℓ increases, the cracks will stabilize at $a/\ell<1$, if the minimum in K (K_{min}) is less than $K_c^{g.b}$ (Fig. 3). The wedge opening at stability h_s can be related to the stable crack length a_s (from Eqn. 1) by;

$$h_s/a_s = (\pi\sigma_n(1-\nu^2)/E)[K_c^{g.b}/\sigma_n\sqrt{\pi(a_s/2)} - 1]. \qquad (3)$$

When K does not decrease (or when $K_{min} > K_c^{g.b}$) the crack will continue

to propagate until it reaches the opposite triple point, where it will stabilize (because the singularity is relaxed by boundary sliding, Fig. 1). The formation of these facet-sized cavities is of greatest current interest, because these are the cavities that primarily contribute to the creep strain and the failure time. The time taken for such cavities to evolve will be addressed in the following section.

4. CRACK PROPAGATION

4.1 General Considerations

A crack will propagate whenever the stress intensity factor K exceeds the critical value $K_c^{g.b}$. The motion of a crack on a susceptible boundary (determined as described in the preceding section) can thus be directly obtained from Eqn. (1) (with K replaced by the critical value), provided that the time dependence of the opening h can be established. The rate of wedge opening h is determined by a conventional spring, dashpot approach; wherein the opening is motivated by the elasticity of the material and resisted by the viscosity η of the sliding boundary (Fig. 4). The wedge opening permitted by the elasticity of the material is governed exclusively by the grain boundary sliding and therefore relates to the resolved shear stress τ_s. The normal stress is not involved because it generates an opening at the crack center but not at the wedge. The problem is most conveniently posed using the illustration shown in Fig. 4. The wedge crack releases the constraint of the surrounding grains on the triple point and the grain on one side of the sliding boundary exerts an elastic force P on the triple point. The initial magnitude of the elastic force, P_o, when the wedge opening

is zero, is related directly to the revolved shear stress τ_s by;

$$P_o = \tau_s \ell b \tag{4}$$

As the crack extends and the wedge opening increases the force decreases, and must reduce to zero at elastic equilibrium, i.e., at the stable value of the elastic wedge opening, h_w. The reduction in force occurs in accord with the linear elastic properties of the grain, such that

$$P/P_o = 1 - h/h_w \tag{5}$$

The average effective shear stress τ_B acting on the boundary at any instant is related to the force P by,

$$P = \tau_B(\ell-h)b \tag{6}$$

Combining Eqns. (4), (5) and (6) the stress τ_B that dictates the sliding becomes (since $h<<\ell$);

$$\tau_B = \tau_s(1-h/h_w) \tag{7}$$

The sliding rate $\dot{u}$ at any location along the boundary is related to the effective local shear stress τ_x by the usual relation

$$\dot{u} = \tau_x \delta_b/\eta \tag{8}$$

where δ_b is the thickness of the boundary. Alternatively, the average sliding rate $\langle\dot{u}\rangle$ can be related to the average effective stress τ_B by;

$$\langle \dot{u} \rangle = \tau_B \delta_b / \eta \tag{9}$$

Combining with Eqn. (7) the average sliding rate becomes

$$\langle \dot{u} \rangle = (\tau_s \delta_b / \eta)(1-h/h_w) \tag{10}$$

In order to relate this result to the wedge opening rate $\dot{h}$, we note that the elastic displacement u of a mode II crack (length 2ℓ) subjected to uniform shear varies with distance x from the center as[21]

$$u(x) = \frac{4\tau_B(1-\nu^2)(\ell^2-x^2)^{\frac{1}{2}}}{\pi E} \tag{11}$$

The average displacement is thus;

$$\langle u \rangle = \tau_B \ell (1-\nu^2)/E \tag{12}$$

and the maximum displacement $\hat{u}$ at the center (x=0) is

$$\hat{u} = 4\tau_B \ell (1-\nu^2)/\pi E = 4\langle u \rangle / \pi \tag{13}$$

where $\hat{u} \equiv h \operatorname{cosec} \phi$. The average sliding displacement $\langle u \rangle$ is thus related to the wedge opening h by

$$\langle u \rangle = \frac{\pi}{4} h \operatorname{cosec} \phi \tag{14}$$

Substituting $\langle u \rangle$ from Eqn. (14) into Eqn. (10), the wedge opening rate becomes

$$\dot{h} = \frac{4 \sin\phi \tau_s \delta_b}{\pi \eta} [1-h/h_w] \tag{15}$$

For the trivial case of constant h_w (independent of time), integration of Eqn. (15) yields the result;

$$h/h_w = 1 - \exp\left[-\frac{4\sin\phi\tau_s\delta_b t}{\pi h_w \eta}\right]$$

$$\equiv 1 - \exp(-t/t_R) \qquad (16)$$

where the relaxation time t_R is;

$$t_R = \pi h_w \eta / 4\tau_s \delta_b \sin\phi$$

Evidently, for those boundaries on which the crack stabilize at $(a/\ell) < 1$, the time taken for the crack to attain its stable length $a_s \to \infty$. This characteristic re-emphasizes the relative insignificance of cracking on these boundaries: with regard to contributions to the creep strain and the failure time. A more significant problem is the propagation time for those cracks that only stabilize when $a \to \ell$; a problem examined in the following section.

4.2 The Propagation Time

The crack propagation under conditions where $K_c^{g.b} < K_{min}$ will exhibit the general characteristics depicted in Fig. 5. The initial growth is constrained by the grain boundary sliding rate. However, when the crack reaches a critical length a*, at which it can continue to propagate at a fixed wedge opening h* (due to the action of the normal stress, σ_n), the constraint imposed by the boundary sliding rate becomes relaxed and the crack will extend catastrophically up to the stable length ℓ. The

propagation time t_p is determined by the time taken for the crack to attain the critical length a*. Hence, t_p can be ascertained if both a* and the driving force for sliding in the range $0 < a < a^*$ can be deduced.

The critical length a* is given by the coupled requirement that K increases with crack length at a fixed wedge opening h, i.e., the crack is driven by the normal stress, and that K at this condition, K*, is equal to $K_c^{g.b}$.† The first condition is established by determining when K for a fixed h is a minimum; because, upon exceeding the minimum, K will increase monotonically with crack length and the crack will become unstable. Hence, differentiating Eqn. (1) with respect to a at fixed h and setting to zero, gives

$$a^* = h^* E/\sigma_n \, \pi(1-\nu^2) \tag{17}$$

Substituting h* from Eqn. (17) into Eqn. (1), and requiring that the resultant $K = K_c^{g.b}$, then gives;

$$a^* = \frac{1}{2\pi} \left[\frac{K_c^{g.b}}{\sigma_n}\right]^2 \tag{18}$$

The equivalent critical wedge opening h*, obtained from Eqn. (1) is;

$$h^* = \frac{(K_c^{g.b})^2 (1-\nu^2)}{2\sigma_n E} \tag{19}$$

---

†The crack growth constrained by the wedge opening always occurs with $K = K_c^{g.b}$; hence, K* cannot exceed $K_c^{g.b}$ until the growth becomes catastrophic.

The equilibrium elastic opening h_w (at which the elastic driving force is zero) is dictated exclusively by the grain boundary sliding and represents the opening at which sliding would cease. The equilibrium opening will depend on both the instantaneous crack length and the in-plane shear stress. It can be ascertained by equating the wedge opening components of Eqn. (1) and Fig. 2, by noting that the wedge opening, K_w, pertinent to Fig. 2 is

$$K_w = \kappa\tau\sqrt{\ell} - \tau_s \sin 2\phi \sqrt{\pi(a/2)} \tag{20}$$

The equilibrium opening then becomes,

$$h_w = \frac{\sqrt{2\pi}(1-\nu^2)a\tau_s}{E} \left[\left(\frac{\kappa\tau(a/\ell,\phi)}{\sqrt{a/\ell}} \right) - \sqrt{\pi/2} \sin 2\phi \right] \tag{21}$$

where K^{τ} is obtained from Fig. 2. The instantaneous wedge opening h prior to catastrophic extension is determined by applying the crack extension requirement ($K = K_c^{g.b}$) to Eqn. (1), giving

$$h = \frac{\sqrt{2\pi}(1-\nu^2)a}{E} \left[\left(K_c^{g.b}/\sqrt{a} \right) - \left(\sqrt{\pi/2}\ \sigma_n \right) \right] \tag{22}$$

Differentiation then yields the opening rate $\dot{h}$, as

$$\dot{h} = \frac{\sqrt{2\pi}(1-\nu^2)\dot{a}}{E} \left[\left(K_c^{g.b}/\sqrt{a} \right) - \left(\sqrt{2\pi}\ \sigma_n \right) \right] \tag{23}$$

Substituting the above results for h, h_w and $\dot{h}$ into Eqn. (15) and re-arranging we obtain

$$\dot{a}(1-\nu^2)\left(\frac{\eta}{E\delta_b}\right) = \frac{4\sin\phi\sqrt{a}}{\pi^2}\left\{\frac{[\sqrt{a}-2\sqrt{a^*}+(\tau_s/\sigma_n)(\kappa\sqrt{2\ell/\pi}-\sqrt{a}\,\sin 2\phi)]}{(\kappa\sqrt{2\ell/\pi}-\sqrt{a}\,\sin 2\phi)(\sqrt{a^*}-\sqrt{a})}\right\} \quad (24)$$

The significant features of Eqn. (24) to note are: (i) there is a threshold for crack development (obtained by setting the numerator to zero) given by the condition $\kappa\tau\sqrt{\ell}|_{a=0} \geq K_c^{g.b}$, (ii) the velocity becomes unbounded as $a \to a^*$, (iii) the velocity above the threshold condition is zero at a = 0. The general trends, exemplified by the plots presented in Fig. 6 (for $\phi = \pi/4$ and $\beta = 1$), are complex. However, some conditions wherein simplified crack velocity relations pertain can be explored by re-expressing Eqn. (24) in terms of a threshold stress, through the term

$$a^*_{th} \equiv \ell(\tau_s/\sigma_n)^2\,\kappa^2/2\pi = (\tfrac{1}{2}\pi)(K_c^{g.b}/\sigma_n)^2_{th}, \quad (25)$$

to obtain;

$$a(1-\nu^2)\left(\frac{\eta}{E\delta_b}\right) = \frac{4\beta\sin\phi(a/a^*)^{\frac{1}{2}}}{\pi^2}\,\frac{[(a/a^*)^{\frac{1}{2}}(1-\beta\sin 2\phi)+2(a^*_{th}/a^*)^{\frac{1}{2}}-2]}{[2(a^*_{th}/a^*)^{\frac{1}{2}}-\beta(a/a^*)^{\frac{1}{2}}\sin 2\phi][1-(a/a^*)^{\frac{1}{2}}]} \quad (26)$$

where $\beta = \tau_s/\sigma_n$. For stresses considerably in excess of the threshold, such that $a^* << a^*_{th}$, and for β values typical of crack-susceptible boundaries ($\beta \sim 1$), Eqn. (26) reduces to;

$$\dot{a}(1-\nu^2)\,(\eta/E\delta_b) \approx 4\sin\phi\beta(a/a^*)^{\frac{1}{2}}/\pi^2[1-(a/a^*)^{\frac{1}{2}}] \quad (27)$$

The early growth is thus dominated by the square root term in the numerator - a deceleartion; while the final stages of growth, dictated by the denominator, are accompanied by a crack acceleration. These trends

are evident in Fig. 6. Also, note that the facet length ℓ does not enter this limit solution.

The time of propagation t_p of a crack across the boundary facet can be obtained by direct integration of the velocity relation. For the limit solution, Eqn. (27), the following simple result obtains;

$$t_p = \frac{\pi(1-\nu^2)}{8\sin\phi} \frac{(K_c^{g.b})^2}{\sigma_n \tau_s} \left(\frac{\eta}{E\delta_b}\right) \tag{28}$$

This result provides useful insights into the relative roles of the important microstructural variables, η, δ_b, $K_c^{g.b}$, ϕ, and of the relative stress conditions σ_n, τ_s. For a uniaxial tension σ^T inclined at an angle ψ to the sliding boundary,

$$\tau_s = \sigma^T \sin\psi \cos\psi,$$

$$\sigma_n = \sigma^T \sin^2(\psi+\phi),$$

Eqn. (28) becomes;

$$t_p = \frac{\pi(1-\nu^2)}{8(\sigma^T)^2} \left[\frac{(K_c^{g.b})^2 \eta}{E\delta_b}\right] \frac{1}{\sin\phi\sin\psi\cos\psi\sin^2(\psi+\phi)} \tag{29}$$

The non-linear stress dependence is significant: a result that essentially derives from the condition that the crack length at critically a* is proportional to the inverse square of the normal stress. Differentiation of Eqn. (29) with respect to ϕ and ψ suggests that the most fracture susceptible boundaries (those with minimum t_p) pertain for the condition $\psi = 35°$, $\phi = 55°$, yielding

$$(t_p)_{min} \sim \left[\frac{K_c^{g.b}}{\sigma^T\sqrt{\delta_b}}\right]^2 \left(\frac{\eta}{E}\right) \qquad (30)$$

A more complete relation for the propagation time derives from Eqn. (24), as

$$t_p = \frac{\pi^2(1-\nu^2)}{4}\left(\frac{\eta}{E}\right)\left(\frac{\ell}{\delta_b}\right) \operatorname{cosec}\phi \int_0^{\alpha^*} \frac{\kappa(\sqrt{2/\pi} - \sqrt{\alpha}\sin 2\phi)(\sqrt{\alpha^*} - \sqrt{\alpha})d\alpha}{\sqrt{\alpha}[\sqrt{\alpha} - 2\sqrt{\alpha^*} + \beta(\kappa\sqrt{2/\pi} - \sqrt{\alpha}\sin 2\phi)]} \qquad (31)$$

where $\alpha = a/\ell$ and $a^* = a^*/\ell$. Some typical results are plotted in Fig. 7. The approximate solution given by Eqn. (28) is also plotted on Fig. 7 to indicate its realm of applicability.

5. IMPLICATIONS

The time of propagation of a crack across a grain facet, given by Eqns. (30) and (31) is the basis for deriving implications concerning the cracking threshold, the creep strain and the failure time. The magnitudes of these quantities depend upon the statistical distributions of grain boundary properties and orientations;[7] properties which are generally unknown at this juncture. Preliminary estimates of the creep response are deduced herein using simplified assumptions concerning the grain boundary properties. More detailed creep predictions await a knowledge of typical statistical properties of grain boundaries.

5.1 The Cracking Threshold

The critical resolved shear stress for crack initiation τ_s^c in the absence of pre-existent triple point voids is simply related to the critical stress intensity factor by;

$$\tau_s^c = K_c^{g.b}/\sqrt{\ell}[\kappa(\phi)|a=0] \qquad (32)$$

indicating dominant influences of the grain size, fracture energy and grain orientations. Noting that $\kappa|_{a=0} \sim 1.4$ (Fig. 2) and taking $K_c^{g.b}$ ~ 0.5 MPa$\sqrt{m}$, the critical resolved stress for a typical grain facet length of 10 μm is ~100 MPa, indicating an applied stress of ~200 MPa. This is a relatively large threshold stress; and an even larger threshold will pertain for fine grained materials, e.g., ~600 MPa for a 1 μm facet length. This conclusion is not significantly modified in the presence of pre-existent voids. (Specifically, for a void of length a_o at the triple point, the critical threshold stress reduces to;

$$\tau_s^c = \frac{[K_c^{g.b} - \sigma_n\sqrt{\pi(a_o/2)}]}{[\kappa\sqrt{\ell} - \sqrt{\pi(a_o/2)}\ \sin 2\phi]} \tag{33}$$

which, for a sliding boundary inclined at $\pi/4$ and the cracking boundary at $\pi/2$ to the applied tensile stress, becomes;

$$\sigma_n^c = \frac{2K_c^{g.b}}{\kappa\sqrt{\ell} + \sqrt{\pi(a_o/2)}}\ , \tag{34}$$

showing that typical pre-existent voids ($a_o \sim 0.1\ell$) exert a negligible influence on the threshold stress). The proposed mode of deformation is therefore most likely to occur in regions of high stress, notably in the vicinity of crack tips. In fact, this mechanism is a possible origin of the high temperature slow crack growth observed in ceramic systems[23].

5.2 The Creep Strain

The creep strain in a material subject to boundary sliding and cracking consists (in the absence of diffusion) of an initial transient,

caused by elastically constrained boundary sliding, followed by an accumulation of strain associated with crack evolution and the concomittant additional boundary sliding. The latter strain is of primary interest herein.

The formation and growth of an isolated crack increases the compliance of a body, by an amount that depends on the crack length and the extent of sliding. Specific relations for the compliance change are avilable for bodies containing arrays of cracks,[22] but analogous results for coupled cracking and sliding have not yet been derived. Equivalent crack morphologies are thus adopted for the estimation of changes in compliance and hence, to obtain the creep strain[7,22];

$$\varepsilon = \frac{\sigma}{E}\left[1 - \frac{16(1-\nu^2)(10-3\nu)}{45(2-\nu)}\ \frac{N}{V}\ \langle a_+^3\rangle\right]^{-1} \qquad (35)$$

where N is the number of cracks in the volume V and a_+ is the radius of the equivalent crack (e.g., a_+ may be taken as the sum of the actual crack length and the length of the contiguous sliding boundary).

Consider first the trivial case, in which all boundaries subject to tension contain cracks. Then, Eqn. (35) becomes (for $\nu \sim 0.2$);

$$\varepsilon \approx \frac{\sigma}{E}\left[1 - \langle(a_+/\ell)^3\rangle\right]^{-1} \qquad (36)$$

This result emphasizes that the creep strains are necessarily small (at most, a few times the elastic strain, σ/E) until virtually all tensile boundaries become fully cavitated. This mechanism should not, therefore, be invoked to explain relatively large creep deformations. (Subsequent to full cavitation, of course, appreciable creep strains, up to ~30%,

can develop at a rate dictated by the grain boundary viscosity (Fig. 8) viz. (Appendix II, Eqn. A10));

$$\dot{\varepsilon} \approx A\sigma\delta_b/\eta\ell$$

where A is a constant in the range 0.5 to 2, depending upon grain morphologies). The strain rate, prior to full cavitation, obtained by by differentiation of Eqn. (36) is;

$$\dot{\varepsilon} = \frac{3\sigma(a_+)^2\dot{a}_+}{E\ell^3[1-\langle a_+/\ell\rangle^3]^2} \tag{37}$$

A detailed analysis of the crack size distribution, as a function of time, is needed in order to relate this strain-rate to the time independent variables. This is beyond the scope of the present paper. However, if all cracks are considered to be similar in length, the time dependence of the crack length, deduced by integrating the simplified crack velocity relation (Eqn. 27),

$$\left(\frac{a}{a^*}\right)^{\frac{1}{2}} = 1 - \left[1 - \frac{4\beta\sin\phi}{\pi^2(1-\nu^2)} \left(\frac{E\delta_b}{\eta a^*}\right) t\right]^{\frac{1}{2}} \tag{38}$$

can be combined with Eqn. (37) to yield an expression for the strain-rate. For the initial stages of creep ($a < a^* < \ell$), the result obtained by setting $a \sim a_+$ is;

$$\dot{\varepsilon} = 6\left(\frac{2\sqrt{2}\beta\sin\phi}{\pi^{3/2}(1-\nu^2)}\right)^6 \left(\frac{E\delta_b}{K_c^{g.b}\eta\sqrt{\ell}}\right)^6 \frac{\sigma^7}{E} t^5 \tag{39}$$

A highly non-linear, time variant, creep strain is thus to be anticipated for conditions which promote the relatively uniform growth of grain boundary cracks.

More generally, cracks can be expected to accumulate as full facet-sized cavities (as relaxed by boundary sliding) on boundaries of diminishing susceptibility. Then, a statistical function (that describes the relative cracking susceptibilities of boundaries within the polycrystalline aggregate) is required to deduce the creep strain. Defining Φ as the cumulative probability that a tensile boundary will have developed a full facet-sized cavity, length ℓ, at time t, the creep strain derives from Eqn. (36) as;

$$\varepsilon \approx \frac{\sigma}{E(1-\Phi)} \tag{40}$$

The strain rate is thus;

$$\dot{\varepsilon} = \frac{\sigma\dot{\Phi}}{E(1-\Phi)^2} \tag{41a}$$

which for $\Phi << 1$ (i.e., small strains) reduces to;

$$\dot{\varepsilon} \approx \sigma\dot{\Phi}/E. \tag{41b}$$

Adopting a previous suggestion that, for small Φ[7],

$$\Phi \sim \left(\frac{t}{t_o}\right)^k \tag{42}$$

where k is a shape parameter and t_o a scale parameter, Eqn. (41b) becomes;

$$\dot{\varepsilon} \approx k\sigma t^{k-1} t_o^{-k} \tag{43}$$

Inserting a value for the scale parameter derived directly from the reduced form of the cavity propagation time t_p (Eqn. 30), the final expression for the creep strain rate becomes;

$$\dot{\varepsilon} = k\lambda_o^k \sigma^{2k+1} t^{k-1} \tag{44}$$

where λ_o is the scale parameter derived from the quantity, $(E\delta_b/\eta K_c^2)$. It is noted that a steady-state creep prevails when the shape parameter k=1, with a stress exponent of three. Otherwise, accelerating or decelerating creep strains are to be anticipated. Further study is needed to specify the microstructural rationale for the choice of the shape parameter, k, and hence, to predict specific creep strain rates.

5.3 The Failure Time

The failure time also depends upon the uniformity of the crack propagation process (amongst the tensile boundaries). For relatively uniform growth, the propagation time t_p anticipated by Eqn. (30) comprises the initial constituent of the failure sequence. This is superseded by unconstrained sliding, which contributes an additional time to the ultimate separation, given by Eqn. (A11). The total failure time is thus;

$$t_f \sim 0.6 \left(\frac{\eta \ell}{\sigma^T \delta_b}\right) \left[1 + \Omega \frac{\left(K_c^{g.b}\right)^2}{E\sigma^T \ell}\right] \equiv 0.6 \left(\frac{\eta \ell}{\sigma^T \delta_b}\right) (1+\omega) \tag{45}$$

where Ω is a coefficient (~5) that depends upon the grain morphologies considered. Since σ^T must exceed the threshold for crack initiation

(Eqn. 34), the maximum possible contribution to t_f obtains by setting σ^T to its threshold value; whereupon;

$$\omega \sim \Omega K_c^{g.b}/E\sqrt{\ell} \tag{46}$$

Inserting typical values for $K_c^{g.b}$ (~1 MPa$\sqrt{m}$), E(4×10^{11}Pa) and ℓ(4×10^{-6}m) indicates that $\omega<10^{-1}$. The failure time is thus dominated by the unconstrained sliding process. This suggests that, for uniform grain structures, failure is adequately represented by Eqn. (A10).

Most microstructures will not exhibit the uniformity demanded by the above anlaysis. A statistical approach to failure is thus more generally applicable. This is a complex problem since interaction effects between cracks on neighboring boundaries are expected to contribute significantly to the failure process. Neglect of interaction effects would suggest a relation[7]

$$\ell n t_f = \ell n t_o - \frac{4\sigma^2 \ell}{\pi k K_c^2} \ell n(4A/\ell^2) \tag{47}$$

where A is the total grain boundary area, K_c is the macrotoughness of the material, k is a shape parameter and t_o a scale parameter (c.f., Eqn. 42). Inserting a value for t_o from Eqn. (30) gives,

$$\ell n t_f = A_o - 2\ell n\sigma - \sigma^2 \left(\frac{4\ell}{k\pi K_c^2}\right) \ell n \left(\frac{4A}{\ell^2}\right) \tag{48}$$

where A_o is the scale parameter connected with the term, $(K_c^{g.b})^2\eta/E\delta_b$. The behavior of this function and its correspondence with fracture data has been discussed elsewhere[7]. The incorporation of interaction

effects would tend to diminish the significance of the final term in Eqn. (48); a term which reflects the product of the survival probabilities of individual grain boundaries.

6. CONCLUSION

A mechanism of creep failure involving grain boundary sliding and brittle cracking has been examined. This mechanism may exist in ceramic materials with relatively planar boundaries, as produced for example in systems prepared by liquid phase sintering. It has been demonstrated that the mechanism requires a relatively high threshold stress and is thus most likely to be observed at intermediate temperatures or in the vicinity of crack tips (viz. a slow crack growth mechanism). An analysis of crack extension across grain boundaries, constrained by the rate of boundary sliding, has been conducted. The analysis has provided implications for creep strain-rates and failure times; the specific results depending upon boundary orientations. In general, both the creep strain-rate and the failure time are non-linear in stress. The important material parameters are the grain boundary viscosity and fracture energy and the grain size.

ACKNOWLEDGMENT

This work was supported in part by the Defense Advanced Research Projects Agency under Contract No. MDA903-76C-0250 with the University of Michigan, and in part by the Department of Energy under Contract No. W-7405-Eng-48.

APPENDIX I

THE STRESS INTENSITY FACTORS FOR A CRACKED DISLOCATION

The change in the mechanical energy ΔU of a system subject to a tensile stress σ, during the formation of a wedge crack of length a and heigth 2h (Fig. 4) that forms normal to the stress is given by;[18]

$$b\Delta U = -\frac{Eh^2}{2\pi(1-\nu^2)} \ell n \left(\frac{4R}{a}\right) - \frac{\pi(1-\nu^2)\sigma^2 a^2}{4E} - \sigma a h \qquad (A1)$$

where b is the sample width and R is an arbitrary field radius. Since the crack can only extend from one end, the strain energy release rate, G, is;

$$G = -\frac{1}{b}\left(\frac{\partial \Delta U}{\partial a}\right)_{\sigma} = \frac{Eh^2}{2\pi(1-\nu^2)a} + \frac{\pi(1-\nu^2)\sigma^2 a}{2E} + \sigma h \qquad (A2)$$

and the stress intensity factor ($K^2 = EG/(1-\nu^2)$) is;

$$K = \left[\frac{(Eh)^2}{2\pi(1-\nu^2)^2 a} + \frac{\pi\sigma^2 a}{2E} + \frac{\sigma E h}{(1-\nu^2)}\right]^{\frac{1}{2}} \qquad (A3)$$

$$= \sigma_n\sqrt{\pi(a/2)} + hE/\sqrt{2\pi a}\,(1-\nu^2) \qquad (A3)$$

Rearranging to obtain the wedge opening gives;

$$\frac{h}{a} = \frac{\pi\sigma(1-\nu^2)}{E}\left[\frac{K}{\sigma\sqrt{\pi(a/2)}} - 1\right] \qquad (A4)$$

Inspection of Eqn. (A3) reveals that it has two components. The first is the solution for a crack subjected to a normal stress ($\sigma_n\sqrt{\pi(a/2)}$)

and the other is due to the wedge opening. This result is consistent with the linear superposition requirement for K. The wedge opening component is also consistent (except for a numerical factor) with the wedge crack solution developed by Barenblatt[24]. A self consistent stress intensity factor solution thus emerges from the cracked dislocation analysis, although a numerical deficiency might be exposed in more detailed anlayses. Note that the normal stress component causes K to increase with crack length; whereas the wedging component requires that K decrease with crack length, when subject to a fixed wedge opening. A minimum in K can thus be anticipated to occur for certain crack extension conditions, as observed, for example, in Fig. 2.

APPENDIX II

STRAIN RATES FOR UNCONSTRAINED SLIDING

When all grain boundaries subject to tensile stress have fully-cavitated (Fig. 8), subsequent deformation is controlled by unconstrained grain boundary sliding. The sliding rate $\dot{\delta}$ is related to the resolved shear stress, τ_B, on the remaining contact area by;

$$\dot{\delta} = \frac{\tau_\beta \delta_b}{\eta} \tag{A5}$$

Noting that the contact area is $\sim\ell(\ell-2\delta)$, Eqn. (A5) becomes

$$\dot{\delta} = 0.43 \frac{\sigma^T \delta_b \ell}{\eta(\ell-2\delta)} \tag{A6}$$

yielding a strain-rate;

$$\dot{\varepsilon} = \frac{0.87\sigma^T \delta_b}{\ell\eta(1-2\varepsilon)} \tag{A7}$$

Solving for the strain gives;

$$2\varepsilon = 1 - [1-3.5\sigma^T \delta_b t/\ell\eta]^{\frac{1}{2}} \tag{A8}$$

which for strains $\lesssim 0.2$ reduces to

$$\varepsilon \approx \frac{0.87\sigma^T \delta_b t}{\ell\eta} - 0.77 \left(\frac{\sigma^T \delta_b t}{\ell\eta}\right)^2 \tag{A9}$$

The corresponding strain-rate is

$$\dot{\varepsilon} \approx \frac{0.87\sigma^T\delta_b}{\ell\eta} - 1.54\left(\frac{\sigma^T\delta_b}{\ell\eta}\right)^2 t \qquad \text{(A10)}$$

Ultimate failure occurs as the displacement $\delta \to \ell/2$. The component of the failure time that derives from the unconstrained boundary sliding t_f^u is thus obtained from Eqn. (A6) as;

$$t_f^u \sim \frac{2.3\eta}{\delta_b \ell \sigma^T} \int_0^{\ell/2} (\ell - 2\delta)d\delta \qquad \text{(A11)}$$

$$= 0.6\left(\frac{\eta\ell}{\sigma^T\delta_b}\right)$$

REFERENCES

1. T.J. Chuang and J.R. Rice, Acta Met. (1973) 21, 1625.
2. V. Vitek, Acta Met. (1978), 26, 1345.
3. M.V. Speight, W.B. Beere and G. Roberts, Mat. Sci. Eng., (1978), 36, 155.
4. T.J. Chuang, K.I. Kagawa, J.R. Rice and L.B. Sills, Acta Met., (1979), 27, 265.
5. R. Raj and M.F. Ashby, Acta Met., 23, (1975) 653.
6. R. Raj and C.H. Dang, Phil. Mag., (1975), 32, 909.
7. A.G. Evans and A. Rana, Acta Met., in press.
8. J.A. Williams, Phil. Mag. (1971), 15, 1289.
9. H.E. Evans, Phil. Mag., (1971), 23, 1101.
10. T.G. Langdon, Phil. Mag. (1971), 23, 945.
11. P.T. Heald and J.A. Williams, Phil. Mag. (1972), 24, 1215.
12. R. Raj and M.F. Ashby, Met. Trans., 2 (1971), 1113.
13. J. Porter and A.G. Evans, to be published.
14. L.K.V. Lou, T.E. Mitchell and A.H. Heuer, Jnl. Amer. Ceram. Soc., (1978), 61, 392.
15. O. Krivanek, T. Shaw and G. Thomas, Jnl. Amer. Ceram. Soc., in press.
16. C.W. Lau and A.S. Argon, Fracture 1977 (Ed. D.M.R. Taplin), Univ. Waterloo Press, Vol. 2, p. 595.
17. A.G. Evans, J.R. Rice and J.P. Hirth, Jnl. Amer. Ceram. Soc., in press.
18. A.N. Stroh, Advnaces in Physics (1957), 6, 418.
19. A.H. Cottrell, Trans. AIME (1958), 212, 197.
20. S.N. Chatterjee, Int'l. Jnl. Solids Structures (1975), 11, 521.
21. B.A. Bilby and J.D. Eshelby, Fracture (Ed. H. Liebowite), Vol. 2, 1968 (Academic Press), p. 101.
22. B. Budiansky and J.O'Connell, Int'l. Jnl. Solids Structures, 12, (1976), 81.
23. A.G. Evans and S.M. Wiederhorn, Jnl. Mater. Sci., (1974), 9, 270.
24. G.I. Barenblatt, Adv. Appl. Mech., (1962), Vol. 7.

FIGURE CAPTIONS

Fig. 1: A schematic indicating the sequence of formation of a facet-sized crack; (a) initiation of a crack at a triple point, (b) crack opening due to grain boundary sliding and subsequent crack extension, (c) final, open crack formed by crack tip relaxation induced by grain boundary sliding.

Fig. 2: The variation of stress intensity factor with crack length and angle, for a kinked crack subject to in-plane shear and small closure tractions.

Fig. 3: A schematic derived from Fig. 2 indicating the critical stress intensity factor and the regions of stable and unstable crack extension.

Fig. 4: A schematic illustrating the elastic driving force for boundary sliding and crack opening and the resistance provided by the grain boundary viscosity.

Fig. 5: A typical variation in relative crack length with time. The initial region is limited by the viscosity of the sliding boundary and is followed by a region of unstable growth.

Fig. 6: The variation in crack velocity with crack length for conditions, $\phi = \pi/4$ and $\beta = 1$.

Fig. 7: Crack propagation times plotted as a function of stress level and angle for a shear ratio $\tau_s/\sigma_n = 1$.

Fig. 8: Sliding controlled deformation in the fully cavitated condition.

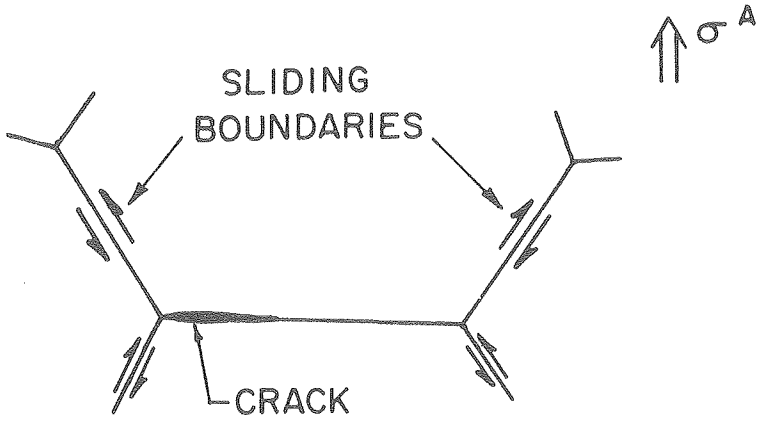

(a) INITIAL CRACK FORMATION

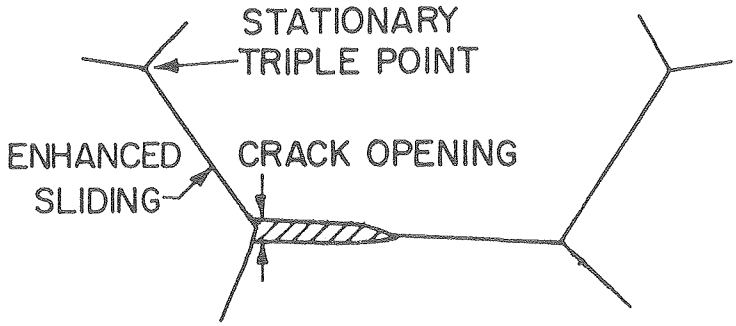

(b) CRACK OPENING BY BOUNDARY SLIDING, FOLLOWED BY ADDITIONAL CRACK EXTENSION

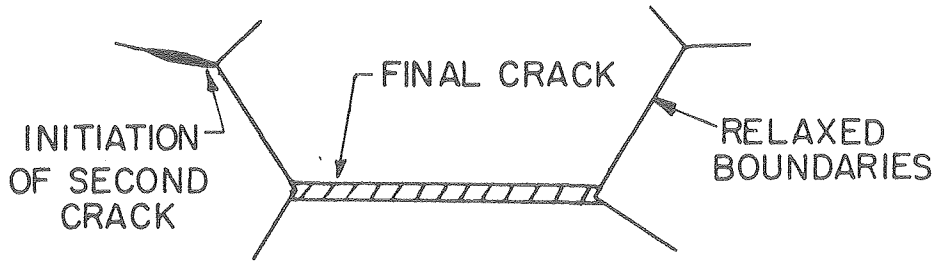

(c) FINAL FACET SIZED CRACK PRODUCED BY SLIDING RELAXATION

XBL 798-6903

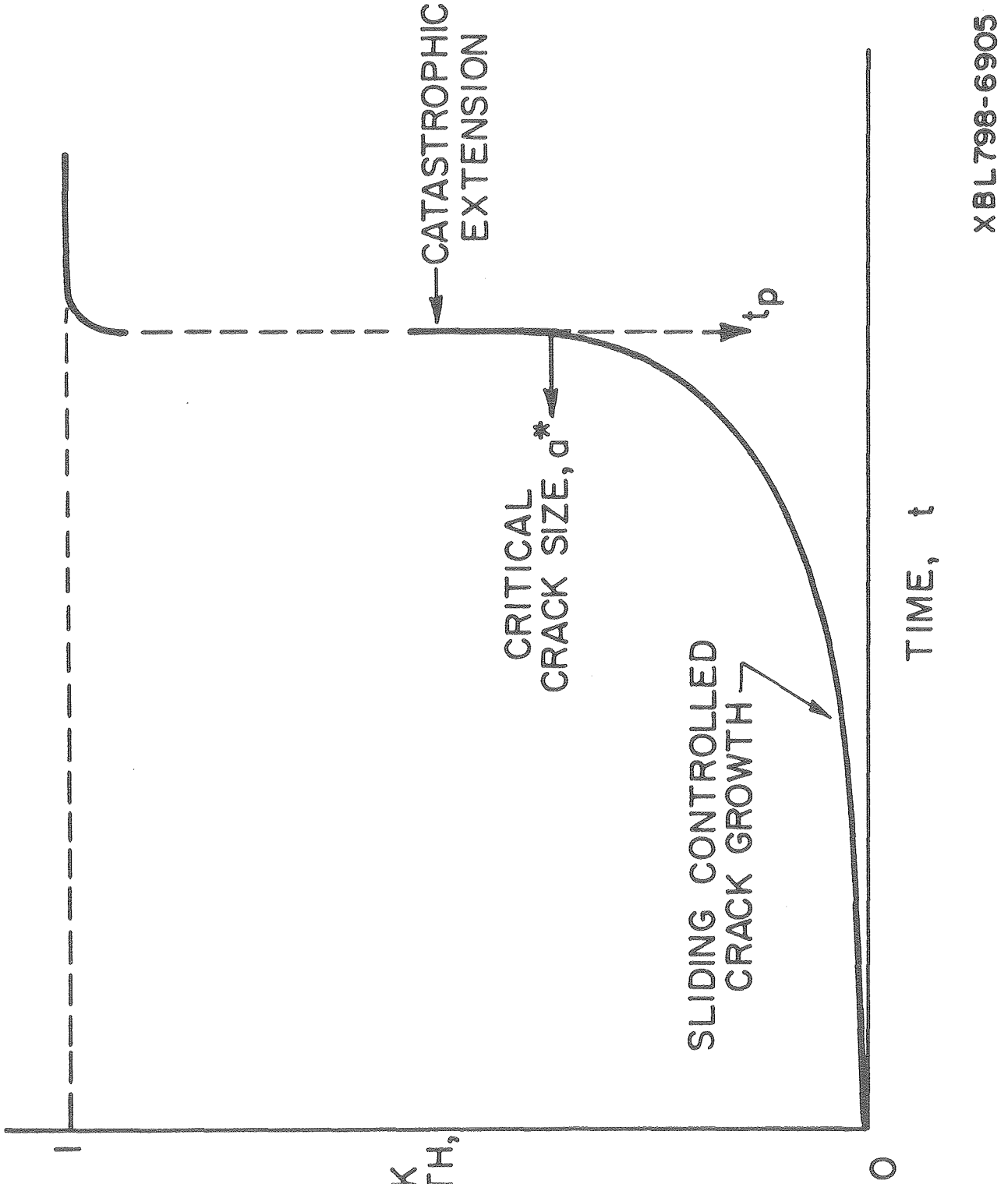
CATASTROPHIC EXTENSION
t_p
CRITICAL CRACK SIZE, a^*
SLIDING CONTROLLED CRACK GROWTH
TIME, t
CRACK LENGTH, a/ℓ
1
0
XBL798-6905

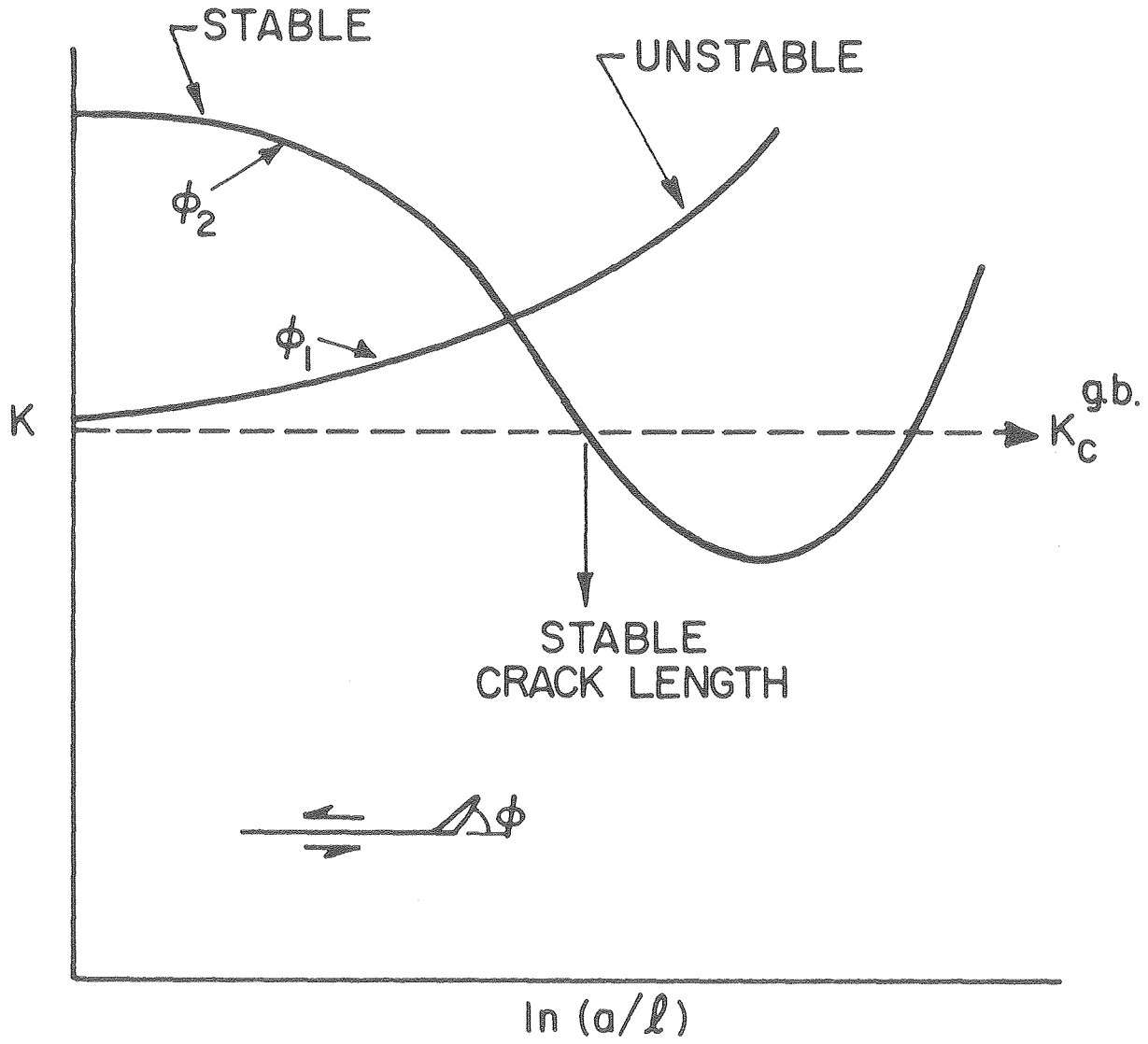
STABLE
UNSTABLE
ϕ_2
ϕ_1
K
$K_c^{g.b.}$
STABLE
CRACK LENGTH
$\Delta\phi$
ln (a/ℓ)

XBL 798-6906

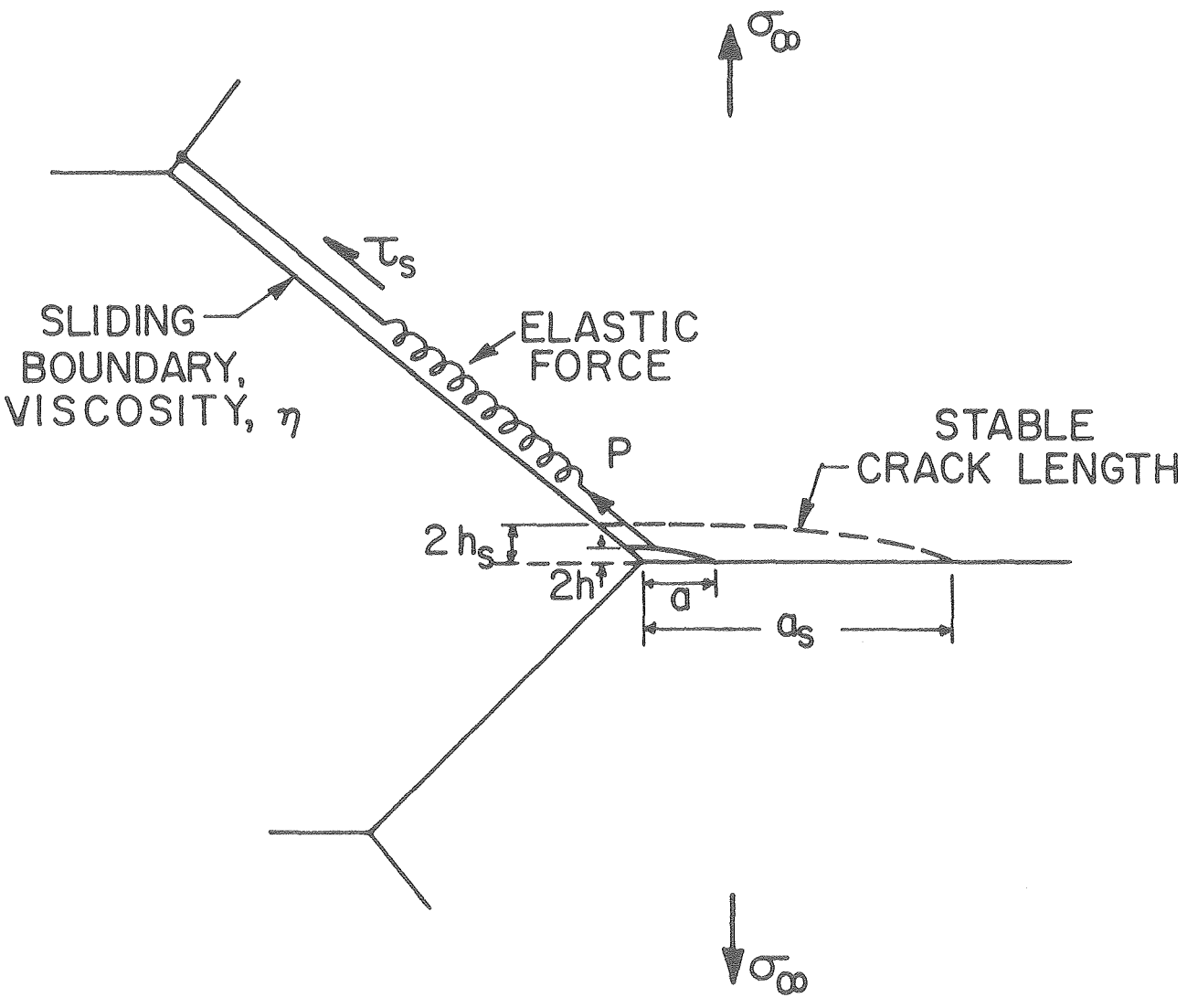
σ_∞
τ_s
SLIDING BOUNDARY, VISCOSITY, η
ELASTIC FORCE
P
STABLE CRACK LENGTH
$2h_s$
$2h$
a
a_s
σ_∞

XBL798-6904

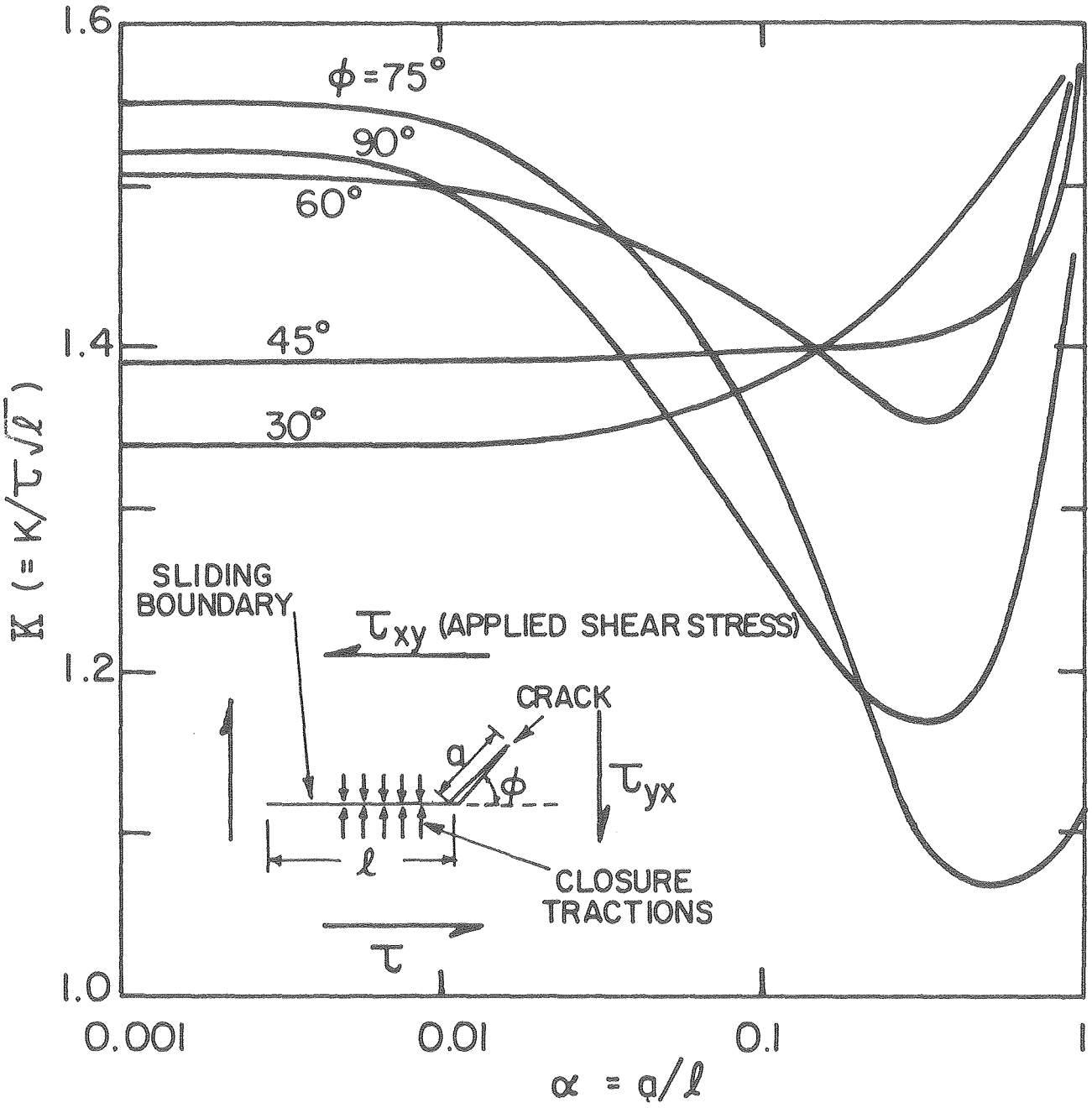
1.6
1.4
1.2
1.0
0.001
0.01
0.1
1
φ = 75°
90°
60°
45°
30°
K (= K/τ√ℓ)
α = a/ℓ
SLIDING BOUNDARY
τxy (APPLIED SHEAR STRESS)
CRACK
a
φ
τyx
ℓ
CLOSURE TRACTIONS
τ

XBL798-6907

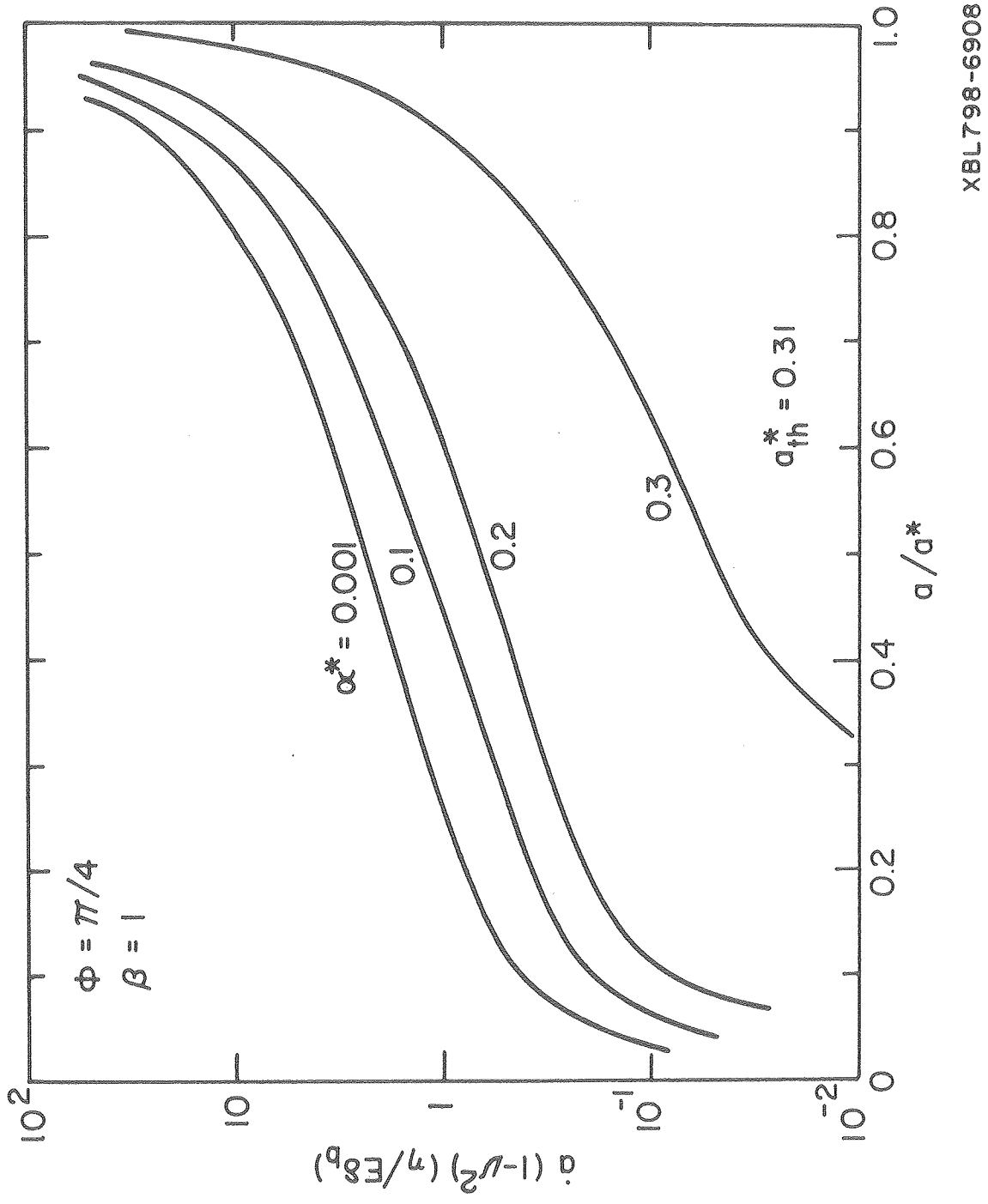
$\dot{a}\ (1-\psi^2)\ (\eta/\varepsilon B_b)$
10^2
10
1
10^{-1}
10^{-2}
0
0.2
0.4
0.6
0.8
1.0
a/a^*
$\Phi = \pi/4$
$\beta = 1$
$\alpha^* = 0.001$
0.1
0.2
0.3
$a^*_{th} = 0.31$

XBL798-6908

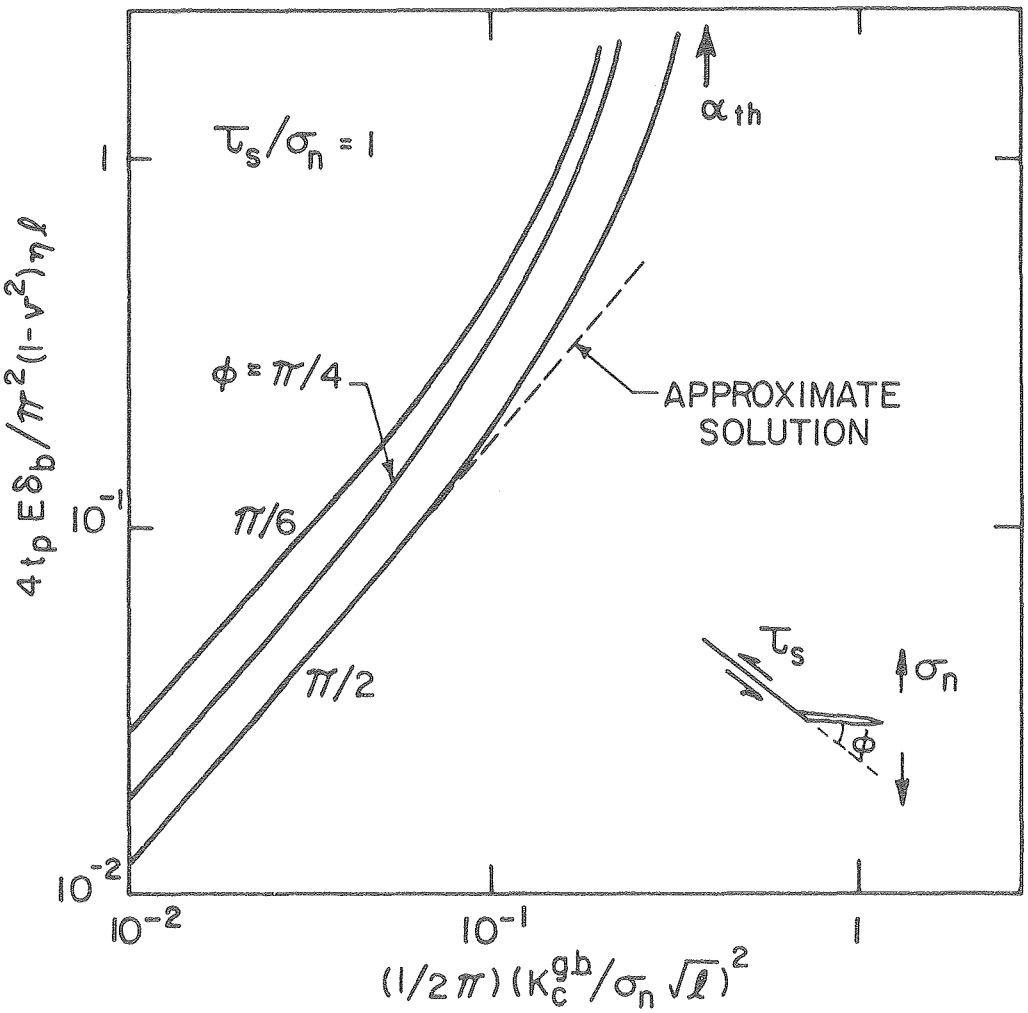
$\tau_s/\sigma_n = 1$
α_{th}
$\phi = \pi/4$
$\pi/6$
$\pi/2$
APPROXIMATE SOLUTION
τ_s
σ_n
ϕ
1
10^{-1}
10^{-2}
10^{-2}
10^{-1}
1
$4tpE\delta_b/\pi^2(1-\nu^2)\eta\ell$
$(1/2\pi)(K_c^{gb}/\sigma_n\sqrt{\ell})^2$

XBL798-6909

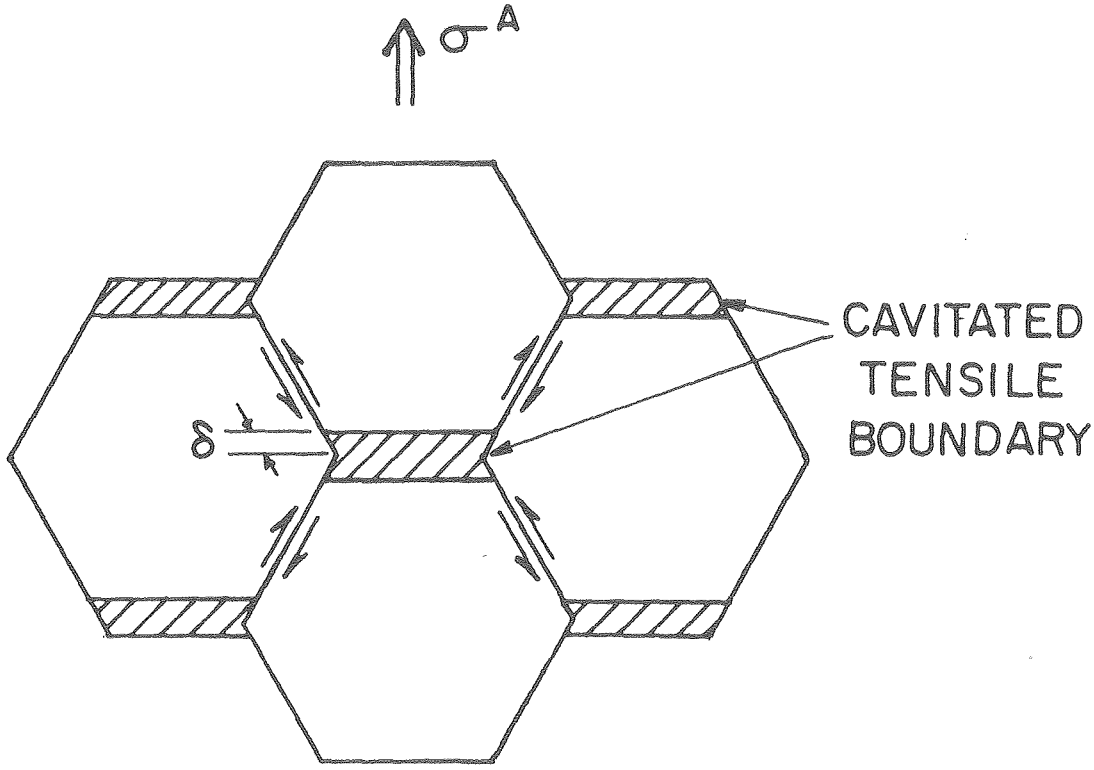

XBL 7911-7280